HHS Public Access

Author manuscript

J Phys Chem C Nanomater Interfaces. Author manuscript; available in PMC 2019 January 28.

Published in final edited form as:

J Phys Chem C Nanomater Interfaces. 2017 November 22; 121(46): 25994–25999. doi:10.1021/acs.jpcc.7b10549.

Imaging of Biomolecular NMR Signals Amplified by Reversible Exchange with Parahydrogen Inside an MRI Scanner

Kirill V. Kovtunov[a,b,*], **Bryce E. Kidd**[c,*], **Oleg G. Salnikov**[a,b], **Liana B. Bales**[c], **Max E. Gemeinhardt**[c], **Jonathan Gesiorski**[c], **Roman V. Shchepin**[g], **Eduard Y. Chekmenev**[d,e,g], **Boyd M. Goodson**[c,f], and **Igor V. Koptyug**[a,b]

[a]International Tomography Center SB RAS, Novosibirsk, 630090, Russia

[b]Novosibirsk State University, Novosibirsk, 630090, Russia

[c]Department of Chemistry and Biochemistry, Southern Illinois University, Carbondale, IL 62901, USA

[d]Department of Biomedical Engineering and Physics, Vanderbilt-Ingram Cancer Center (VICC), Nashville, TN 37232, USA

[e]Russian Academy of Sciences, Moscow, 119991, Russia

[f]Materials Technology Center, Southern Illinois University, Carbondale, IL 62901, USA

[g]Vanderbilt Institute of Imaging Science (VUIIS), Department of Radiology, Vanderbilt University Medical Center, Nashville, TN 37232, USA

Abstract

The Signal Amplification by Reversible Exchange (SABRE) technique employs exchange with singlet-state parahydrogen to efficiently generate high levels of nuclear spin polarization. Spontaneous SABRE has been shown previously to be efficient in the milli-Tesla and micro-Tesla regimes. We have recently demonstrated that high-field SABRE is also possible, where proton sites of molecules that are able to reversibly coordinate to a metal center can be hyperpolarized directly within high-field magnets, potentially offering the convenience of *in situ* hyperpolarization-based spectroscopy and imaging without sample shuttling. Here, we show efficient polarization transfer from parahydrogen (*para*-H_2) to the ^{15}N atoms of imidazole-$^{15}N_2$ and nicotinamide-^{15}N achieved via high-field SABRE (HF-SABRE). Spontaneous transfer of spin order from the *para*-H_2 protons to ^{15}N atoms at the high magnetic field of an MRI scanner allows one not only to record enhanced ^{15}N NMR spectra of *in situ* hyperpolarized biomolecules, but also to perform imaging using conventional MRI sequences. 2D ^{15}N MRI of high-field SABRE-hyperpolarized imidazole with spatial resolution of 0.3×0.3 mm^2 at 9.4 T magnetic field and a high signal-to-noise ratio (SNR) of ~99 was demonstrated. We show that ^{1}H MRI of *in situ* HF-SABRE hyperpolarized biomolecules (*e.g.* imidazole-$^{15}N_2$) is also feasible. Taken together, these

[*]Corresponding Author, kovtunov@tomo.nsc.ru, bryce.kidd@siu.edu.

Notes

The authors declare no competing financial interests.

results show that heteronuclear (^{15}N) and ^{1}H spectroscopic detection and imaging of high-field-SABRE-hyperpolarized molecules are promising tools for a number of emerging applications.

INTRODUCTION

Despite being powerful tools for studying structure, function, metabolism, and dynamics, magnetic resonance imaging and spectroscopic methods suffer from an inherently low internal sensitivity due to weak nuclear spin polarization. NMR hyperpolarization enhances nuclear spin polarization by several orders of magnitude by producing non-Boltzmann distribution of populations of nuclear spin states.[1,2] This massive enhancement of nuclear spin polarization results in corresponding gains in NMR signal intensity.[3–5] A significant amount of work has been directed towards hyperpolarization method development to overcome the sensitivity limitations of conventional magnetic resonance.[6–8] As a result, a number of hyperpolarization techniques have been undergoing rapid development including Dynamic Nuclear Polarization (DNP),[9–11] Spin Exchange Optical Pumping (SEOP),[12,13] Parahydrogen-Induced Polarization (PHIP)[14–16], and Signal Amplification By Reversible Exchange (SABRE).[3,17]

The main drawback of most hyperpolarization approaches is the requirement of complex and costly hardware. In contrast, SABRE and PHIP techniques are based on the use of parahydrogen,[18] production of which is relatively straightforward and inexpensive. The SABRE technique has been pioneered by Duckett and co-workers relatively recently;[3,19,20] it relies on parahydrogen (*para*-H_2) chemical exchange rather than irreversible pairwise parahydrogen addition required to observe PHIP. As a result, the to-be-hyperpolarized compound retains structural integrity throughout the SABRE hyperpolarization process.

In a typical SABRE experiment, *para*-H_2 is bubbled through a solution containing a metal-hydride-based inorganic complex, where *para*-H_2 and the to-be-hyperpolarized substrate exchange simultaneously. To achieve spontaneous transfer of spin order from parahydrogen-derived hyperpolarized (HP) protons to the nuclei of the substrate compound, the solution is normally placed in a magnetic field matched to the spin-spin couplings between the hydride protons and the target nuclei. Thus, spontaneous transfer of nuclear spin order to heteronuclei occurs efficiently at magnetic fields less than Earth's field (less than ca. 1μT), which can be conveniently achieved by the use of a mu-metal shield; this approach is known as SABRE-Shield Enables Alignment Transfer to Heteronuclei (or SABRE-SHEATH).[21] By comparison, matching magnetic fields of a few milli-Tesla have been shown to be the most efficient for SABRE hyperpolarization of substrate protons.[22] SABRE-SHEATH has been shown to hyperpolarize a wide range of nuclei to date (^{15}N, ^{31}P, ^{19}F, ^{13}C, and others)[21,23–26], and it also has been useful for creating HP singlet states, where two or more coupled nuclear spins retain singlet-like behavior in the to-be-hyperpolarized compound.[24,27] Such molecules may be advantageous in the context of increasing the lifetime of the HP states – a property that would be particularly highly valued in biomedical applications, because it would expand the lifetime of HP compounds acting as *in vivo* contrast agents.

^{15}N SABRE-SHEATH hyperpolarization has garnered recent attention because nitrogen is found in a number of biomolecular motifs and ^{15}N sites can have long exponential decay

constants T_1 and T_S (>20 min.); as a result, a number of different SABRE-hyperpolarized ^{15}N-based agents with potentially long hyperpolarization lifetimes[27,28] may be envisioned. Indeed, ^{15}N hyperpolarization of >20% has recently been demonstrated, corresponding to signal enhancement of more than 200,000-fold at 3 T.[29] While ^{15}N HP compounds have great promise for in vivo molecular imaging,[30–32] currently ^{15}N MRI is rare, and to date only low-resolution 2D projection ^{15}N MR imaging (2 × 2 mm^2 in-plane spatial resolution) has been shown in the context of the ^{15}N SABRE and DNP hyperpolarization—in studies involving compounds *without* biological relevance.[21,30] Similarly, the first demonstration of High-Field SABRE (HF-SABRE) was shown for pyridine protons (^{1}H), where spontaneous polarization transfer occurs during *para*-H_2 bubbling through a solution containing an activated SABRE catalyst.[33] Later, it was also shown that spontaneous polarization of ^{15}N sites within pyridine-^{15}N can occur during HF-SABRE.[34,35] However, despite the observation of such signal enhancements, the absolute values for the ^{15}N hyperpolarization that was achieved were relatively low, and prior studies were limited to non-biological compounds like pyridine—an ideal model system for fundamental studies of SABRE processes, but of little interest for biological and biomedical applications.

While HF-SABRE is generally less efficient than SABRE or SABRE-SHEATH occurring in matched milli- or micro-Tesla regimes, HF-SABRE is of interest because it eliminates the need for sample shuttling from the site of a weak matching field to the NMR/MRI detector (where the field is strong). As a result, acquisition of multi-dimensional NMR spectra (in the context of structural and functional biomolecular studies of large macromolecules) can potentially be enabled where the sample is rapidly re-hyperpolarized[36] for each detection event. Moreover, the catalyst activation process and % polarization of biomolecules (which may be employed as hyperpolarized contrast agents) can be monitored via *in situ* detection of hyperpolarized signatures,[37,38] providing a convenient means of process monitoring and quality assurance (QA)—critical components of biomedical translation of hyperpolarized contrast agents.[39] In this paper, we report on ^{15}N HF-SABRE polarization of biologically relevant molecules, imidazole-$^{15}N_2$ and nicotinamide-^{15}N, which can be potentially used as contrast agents for metabolic imaging. Significant signal enhancement of ^{15}N and ^{1}H enables high spatial resolution 2D MRI for the first time for both biomolecules.

RESULTS AND DISCUSSION

For the observation of high-field transfer of spin order from parahydrogen-derived protons to ^{15}N of imidazole-$^{15}N_2$ and nicotinamide-^{15}N, *in situ* bubbling (30 mL·min^{-1}) of 90%-enriched parahydrogen was performed through a SABRE catalyst solution (100 mM of U-^{15}N-enriched imidazole or ^{15}N-enriched nicotinamide and 10 mM of activated IrCl(COD)(IMes) (IMes = 1,3-bis(2,4,6-trimethylphenyl)imidazol-2-ylidene; COD = cyclooctadiene) catalyst in CD_3OD. Unlike in SABRE-SHEATH, simultaneous bubbling of parahydrogen and acquisition of ^{15}N NMR spectra was performed at high magnetic field (7 T) within a MRI scanner (Figure 1).

As expected from similar experiments with pyridine-^{15}N,[34,35,40] HF-SABRE leads to spontaneous transfer of spin order from *para*-H_2-derived protons to ^{15}N spins of imidazole-$^{15}N_2$ (Figure 2) and nicotinamide-^{15}N (Figure 3). Qualitatively different behavior

is observed with the two substrates: In the case of nicotinamide-^{15}N, the catalyst-bound ^{15}N resonance/species is predominantly hyperpolarized (Figure 3b), which is consistent with previous observations for compounds carrying a single ^{15}N spin label (but may also reflect differences in binding kinetics among the substrates).[35] However in the case of imidazole-$^{15}N_2$, which carries two ^{15}N spin labels, the two sites in the catalyst-bound state (i.e. the state relevant for spontaneous polarization transfer) can be overpopulated in a manner analogous to singlet state overpopulation (Figure 2), which is likely the case here—giving rise to a larger HF-SABRE effect. We note that when the catalyst complex is dissociated, both ^{15}N sites of HP imidazole-$^{15}N_2$ resonate at the same frequency due to fast proton exchange[32] (Figure 2b). This ^{15}N HF SABRE of HP contrast agents bearing multiple ^{15}N atoms (and potentially other spin labels[24,36]) could be useful in the context of quality assurance of contrast agents for this and other demonstrated SABRE targets (*e.g.* diazirines[27] and metronidazole[29]), as well as for other emerging biomolecules of interest.

These results are significant in that they allow continuous hyperpolarization at high fields, eliminate relaxation losses during transfer, and dramatically decrease experimental time—as well as demonstrate the other advantages discussed above. Moreover, hyperpolarization detection via conventional SABRE[3] or SABRE-SHEATH[17] with a single 90°-pulse in NMR detectors destroys the hyperpolarized state; however, in the present HF-SABRE method hyperpolarization is continuously refreshed, allowing many 90°-rf-pulses to be applied as desired for multidimensional NMR spectroscopic or imaging applications. For example, here we demonstrate ^{15}N NMR of HP imidazole-$^{15}N_2$ using 32 acquisitions (i.e. with 32 rf excitation pulses) with a total experiment time of 32 s. This experiment represents a massive reduction in acquisition time when compared to a hypothetical experiment employing the ^{15}N signal of thermally polarized imidazole (same concentration) recorded with approximately 1.6×10^6 acquisitions and a total scan time of approximately 19 days. The direct comparison of thermal and hyperpolarized ^{15}N signals allows us to estimate the minimum ^{15}N signal enhancement of ~120.

^{15}N NMR of HP nicotinamide-^{15}N[41] was performed similarly (Figure 3); imaging of the catalyst-bound pool of substrate molecules was also performed (see below in Figure 4). For Figure 3, the same order of ^{15}N signal enhancement was estimated (~100) as was obtained for imidazole-$^{15}N_2$. However, in the case of bound molecules it is difficult to precisely quantify their concentration in solution. Therefore the concentration of bound molecules was simply estimated as being equal to double the concentration of Ir catalyst centers for the signal enhancement estimation. Imaging the catalyst-bound component is also important: Whereas in the case of SABRE with homogenous catalysts the signal distribution is expected to be uniform throughout the length of the hyperpolarization reservoir (e.g. the NMR tube employed here), imaging of heterogeneous catalyst beds may be useful for future optimization of heterogeneous catalyst performance.[42,43]

We also note that to achieve the hyperpolarization-enhanced MR imaging shown in this work, we needed only to employ a common and commercially available imaging pulse sequence and software available on most MRI scanners. Since the HP ^{15}N NMR line shape is antiphase (Figures 2,3), the use of some rf pulse sequences may be challenging due to net cancelation of the positive and negative components of the NMR signal. However, the

FLASH (Fast Low Angle SHot)[44] imaging pulse sequence was successfully applied previously for ^{1}H MRI of 1-hexene under hydrogenation in high magnetic field (PASADENA)[14] conditions (which also gives rise to HP antiphase line shapes[45]). Thus, the present studies utilized the FLASH sequence[46,47] to acquire HP ^{15}N MRI during HF-SABRE of both imidazole-$^{15}N_2$ and nicotinamide-^{15}N (Figure 4).

High-resolution and high SNR 2D ^{15}N MR images of HP biomolecules were demonstrated in this work for the first time, which was possible via the use of HF-SABRE using the standard FLASH pulse sequence. Note that a standard 25-mm i.d. ^{15}N/^{1}H Bruker MRI probe was used in combination with a 5 mm NMR tube (containing a 1/16” Teflon capillary for parahydrogen, leading to a suboptimal rf coil filling factor; thus even higher SNR values can be obtained by optimizing the experimental setup or using a smaller i.d. MRI probe in the context of quality assurance (QA) of contrast agent development and preparation. Moreover, the same rf coil and imaging platform could also be employed for future in vivo studies: i.e. agent QA and in vivo imaging could be performed using the same set of tools, which is critical in the context of biomedical applications—as has been recently discussed by Hovener and co-workers.[48]

The creation of hyperpolarization for heteronuclei of biomolecules via the present approach may also be promising for the production of a continuous flow of HP substrates. Moreover, the HF-SABRE approach requires neither magnetic shields, variable fields, nor specialized RF pulse sequences to achieve polarization transfer,[49] thus allowing this method to be more broadly applicable. To the best of our knowledge, the obtained spatial resolution of 0.31×0.31 mm^2 is the highest reported to date (and ~40-fold better than the previous report[21] on non-biologically relevant compounds) for ^{15}N-detected MRI of any substance, demonstrating the feasibility of high-resolution and high-SNR imaging of this low-gamma nucleus. Indeed, the high-resolution imaging allowed visualization of the Teflon capillary with 1.5 mm o.d. (e.g. Figure 4, top-left). It should be noted that all attempts to perform ^{15}N MRI of the same sample without hyperpolarization by increasing the number of acquisitions and repetition delay were unsuccessful.

We also explored the feasibility of performing ^{1}H imaging enhanced via HF-SABRE (Figure 5, left column). The HF-SABRE method was used for ^{1}H MRI of imidazole-$^{15}N_2$ (using the same sample employed for ^{15}N MRI shown above) and was compared to the ^{1}H MRI of thermally polarized molecules (Figure 5, right column). It should be noted that because of susceptibility distortions, acquisition of ^{1}H MRI was not possible during bubbling—in contrast to ^{15}N MRI shown above; therefore the FLASH pulse sequence was applied with a single acquisition upon termination of *para*-H_2 bubbling. It was shown that for ^{1}H MRI the SNR is improved by at least 3-fold using the HF-SABRE method.

Finally, it is well known that the polarization achieved via SABRE strongly depends not only upon the relevant spin–lattice relaxation time constant (T_1), but also on the presence of quadrupolar nuclei (e.g., ^{14}N, I=1) in the site binding to the Ir-metal center of SABRE catalysts.[25] Therefore, ^{14}N imidazole (with natural abundance of ^{15}N nuclei, ~0.36%) and $^{15}N_2$-enriched imidazole[40] were compared by the HF-SABRE approach. As before, ^{1}H MR

images (Figure 6) of both ^{15}N and ^{14}N imidazole samples were obtained using the FLASH pulse sequence.

Based on the data shown in Figure 6, it may be concluded that no significant differences in ^{1}H polarization efficiency can be observed between $^{15}N_2$-enriched imidazole and imidazole with natural abundant ^{15}N nuclei (i.e. with quadrupolar ^{14}N predominantly located at the nitrogen sites) when using the HF-SABRE method. Therefore, ^{1}H MRI of HF-SABRE HP substrates is free from the requirement to use labeled compounds with isotopically-enriched heteronuclei.

CONCLUSION

In conclusion, it was shown that the HF-SABRE method can be used to spontaneously transfer spin order from continuously bubbling *para*-H_2 to imidazole-$^{15}N_2$ and nicotinamide-^{15}N within an MRI magnet, thereby enabling enhanced ^{15}N MR spectroscopy and high-resolution imaging of biomolecules in solution. Such polarization transfer not only allows efficient acquisition of enhanced ^{15}N NMR spectra *in situ* with signal enhancements ≥ 120 (imidazole) and ≥ 100 (bound nicotinamide) but also enabled improved MRI: Utilization of the standard (and ubiquitous) MRI FLASH pulse sequence in conjunction with the HF-SABRE method afforded rapid acquisition of 2D ^{15}N MRI for imidazole and nicotinamide. High spatial resolution (0.31×0.31 mm^2 for imidazole) and a SNR of ~99 at 9.4 T represents the best reported to date and extends the field to possible MRI applications, and opens the door for pre-clinical studies as well as corresponding efforts with other heteronuclei (e.g. ^{13}C, ^{31}P, ^{19}F, etc.). To verify the utility of the HF-SABRE technique for ^{1}H MRI, the FLASH pulse sequence was used for both thermally polarized and HP imidazole. It was shown that the present approach provides a 3-fold higher SNR. Finally, it was shown that quadrupolar relaxation of ^{14}N is not an issue for ^{1}H MRI polarized via the HF-SABRE method. Taken together, these results show that heteronuclear (^{15}N) and proton (^{1}H) MRI of biomolecules hyperpolarized directly at high magnetic field is promising for various biomedical applications.

ACKNOWLEDGMENT

KVK and OGS thank the Russian Science Foundation (grant 17–73-20030) for the support of ^{15}N MRI experiments, and Alexey Romanov, Alexandra Svyatova (ITC) for helping with images reconstruction, and Larisa M. Kovtunova (BIC) for SABRE catalyst synthesis. The US team thanks the financial support of NIH 1R21EB018014 and 1R21EB020323, NSF CHE-1416268 and CHE-1416432, DOD CDMRP W81XWH-12–1-0159/BC112431, W81XWH-15–1-0271 and W81XWH-15–1-0272, and SIUC MTC and OSPA. OGS acknowledges Haldor Topsøe A/S for the PhD scholarship.

REFERENCES

(1). Nikolaou P; Goodson BM; Chekmenev EY NMR Hyperpolarization Techniques for Biomedicine. Chem. - A Eur. J 2015, 21 (8), 3156–3166.

(2). Barskiy DA; Coffey AM; Nikolaou P; Mikhaylov DM; Goodson BM; Branca RT; Lu GJ; Shapiro MG; Telkki V; Zhivonitko VV; et al. NMR Hyperpolarization Techniques of Gases. Chem. - A Eur. J 2017, 23, 725–751.

(3). Adams RW; Aguilar JA; Atkinson KD; Cowley MJ; Elliott PIP; Duckett SB; Green GGR; Khazal IG; López-Serrano J; Williamson DC Reversible Interactions with Para-Hydrogen Enhance NMR Sensitivity by Polarization Transfer. Science 2009, 323 (5922), 1708–1711. [PubMed: 19325111]

(4). Lloyd LS; Asghar A; Burns MJ; Charlton A; Coombes S; Cowley MJ; Dear GJ; Duckett SB; Genov GR; Green GGR; et al. Hyperpolarisation through Reversible Interactions with Parahydrogen. Catal. Sci. Technol 2014, 4 (10), 3544–3554.

(5). Cowley MJ; Adams RW; Atkinson KD; Cockett MCR; Duckett SB; Green GGR; Lohman JAB; Kerssebaum R; Kilgour D; Mewis RE Iridium N-Heterocyclic Carbene Complexes as Efficient Catalysts for Magnetization Transfer from Para-Hydrogen. J. Am. Chem. Soc 2011, 133 (16), 6134–6137. [PubMed: 21469642]

(6). Geraldes CFGC; Laurent S Classification and Basic Properties of Contrast Agents for Magnetic Resonance Imaging. Contrast Media Mol Imaging 2009, 4 (1), 1–23. [PubMed: 19156706]

(7). Ardenkjær-Larsen JH; Fridlund B; Gram A; Hansson G; Hansson L; Lerche MH; Servin R; Thaning M; Golman K Increase in Signal-to-Noise Ratio of > 10,000 Times in Liquid-State NMR. Proc. Natl. Acad. Sci 2003, 100 (18), 10158–10163. [PubMed: 12930897]

(8). Golman K; Zandt R. in't; Lerche M; Pehrson R; Ardenkjaer-Larsen JH Metabolic Imaging by Hyperpolarized 13C Magnetic Resonance Imaging for In vivoTumor Diagnosis. Cancer Res 2006, 66 (22), 10855–10860. [PubMed: 17108122]

(9). Ardenkjaer-Larsen JH On the Present and Future of Dissolution-DNP. J. Magn. Reson 2016, 264, 3–12. [PubMed: 26920825]

(10). Comment A Dissolution DNP for in Vivo Preclinical Studies. J. Magn. Reson 2016, 264, 39–48. [PubMed: 26920829]

(11). Lee JH; Okuno Y; Cavagnero S Sensitivity Enhancement in Solution NMR: Emerging Ideas and New Frontiers. J. Magn. Reson 2014, 241 (1), 18–31. [PubMed: 24656077]

(12). Goodson BM Nuclear Magnetic Resonance of Laser-Polarized Noble Gases in Molecules, Materials, and Organisms. J. Magn. Reson 2002, 155, 157–216. [PubMed: 12036331]

(13). Schroder L Xenon for NMR Biosensing - Inert but Alert. Phys. Medica 2013, 29, 3–16.

(14). Bowers CR; Weitekamp DP Parahydrogen and Synthesis Allow Dramatically Enhanced Nuclear Alignment. J. Am. Chem. Soc 1987, 109 (18), 5541–5542.

(15). Bowers CR Sensitivity Enhancement Utilizing Parahydrogen. Encycl. Magn. Reson 2007, 9, 4365–4384.

(16). Duckett SB; Wood NJ Parahydrogen-Based NMR Methods as a Mechanistic Probe in Inorganic Chemistry. Coord. Chem. Rev 2008, 252 (21–22), 2278–2291.

(17). Theis T; Truong ML; Coffey AM; Shchepin RV; Waddell KW; Shi F; Goodson BM; Warren WS; Chekmenev EY Microtesla SABRE Enables 10% Nitrogen-15 Nuclear Spin Polarization. J. Am. Chem. Soc 2015, 137 (4), 1404–1407. [PubMed: 25583142]

(18). Green R. a.; Adams RW; Duckett SB; Mewis RE; Williamson DC; Green GGR The Theory and Practice of Hyperpolarization in Magnetic Resonance Using Parahydrogen. Prog. Nucl. Magn. Reson. Spectrosc 2012, 67, 1–48. [PubMed: 23101588]

(19). Atkinson KD; Cowley MJ; Elliott PIP; Duckett SB; Green GGR; López-Serrano J; Whitwood AC Spontaneous Transfer of Parahydrogen Derived Spin Order to Pyridine at Low Magnetic Field. J. Am. Chem. Soc 2009, 131 (37), 13362–13368. [PubMed: 19719167]

(20). Atkinson KD; Cowley MJ; Duckett SB; Elliott PIP; Green G; Lopez-Serrano J; Khazal IG; Whitwood AC SI: Para-Hydrogen Induced Polarisation without Incorporation of Para-Hydrogen into the Analyte. Inorg. Chem 2009, 48 (2), 663–670. [PubMed: 19072592]

(21). Truong ML; Theis T; Coffey AM; Shchepin RV; Waddell KW; Shi F; Goodson BM; Warren WS; Chekmenev EY ^{15}N Hyperpolarization by Reversible Exchange Using SABRE-SHEATH. J. Phys. Chem. C 2015, 119 (16), 8786–8797.

(22). Fekete M; Bay O; Duckett SB; Hart S; Mewis RE; Pridmore N; Rayner PJ; Whitwood A Iridium(III) Hydrido N − Heterocyclic Carbene − Phosphine Complexes as Catalysts in Magnetization Transfer Reactions. Inorg. Chem 2013, 52, 13453–13461. [PubMed: 24215616]

(23). Zhivonitko VV; Skovpin IV; Koptyug IV Strong 31P Nuclear Spin Hyperpolarization Produced via Reversible Chemical Interaction with Parahydrogen. Chem. Commun 2015, 51 (13), 2506–2509.

(24). Zhou Z; Yu J; Colell JFP; Laasner R; Logan A; Barskiy DA; Shchepin RV; Chekmenev EY; Blum V; Warren WS; et al. Long-Lived 13C2 Nuclear Spin States Hyperpolarized by

Parahydrogen in Reversible Exchange at Microtesla Fields. J. Phys. Chem. Lett 2017, 8 (13), 3008–3014. [PubMed: 28594557]

(25). Barskiy DA; Shchepin RV; Tanner CPN; Colell JFP; Goodson BM; Theis T; Warren WS; Chekmenev EY The Absence of Quadrupolar Nuclei Facilitates Efficient 13C Hyperpolarization via Reversible Exchange with Parahydrogen. ChemPhysChem 2017, 18 (12), 1493–1498. [PubMed: 28517362]

(26). Shchepin RV; Goodson BM; Theis T; Warren WS; Chekmenev EY Toward Hyperpolarized 19F Molecular Imaging via Reversible Exchange with Parahydrogen. ChemPhysChem 2017, 18 (15), 1961–1965. [PubMed: 28557156]

(27). Theis T; Ortiz GX; Logan AWJ; Claytor KE; Feng Y; Huhn WP; Blum V; Malcolmson SJ; Chekmenev EY; Wang Q; et al. Direct and Cost-Efficient Hyperpolarization of Long-Lived Nuclear Spin States on Universal 15N2-Diazirine Molecular Tags. Sci. Adv 2016, 2 (3), e1501438–e1501438. [PubMed: 27051867]

(28). Nonaka H; Hata R; Doura T; Nishihara T; Kumagai K; Akakabe M; Tsuda M; Ichikawa K; Sando S A Platform for Designing Hyperpolarized Magnetic Resonance Chemical Probes. Nat Commun 2013, 4, 2411. [PubMed: 24022444]

(29). Barskiy DA; Shchepin RV; Coffey AM; Theis T; Warren WS; Goodson BM; Chekmenev EY Over 20% 15N Hyperpolarization in under One Minute for Metronidazole, an Antibiotic and Hypoxia Probe. J. Am. Chem. Soc 2016, 138 (26), 8080–8083. [PubMed: 27321159]

(30). Jiang W; Lumata L; Chen W; Zhang S; Kovacs Z; Sherry AD; Khemtong C Hyperpolarized 15N-Pyridine Derivatives as pH-Sensitive MRI Agents. Sci. Rep 2015, 5, 9104. [PubMed: 25774436]

(31). Cudalbu C; Comment A; Kurdzesau F; Heeswijk RB; Uffmann K; Jannin S; Denisov V; Kirike D; Gruetter R Feasibility of in Vivo 15N MRS Detection of Hyperpolarized 15N Labeled Choline in Rats. Phys. Chem. Chem. Phys 2010, 12, 5818–5823. [PubMed: 20461252]

(32). Shchepin RV; Barskiy DA; Coffey AM; Theis T; Shi F; Warren WS; Goodson BM; Chekmenev EY 15N Hyperpolarization of Imidazole-15N2 for Magnetic Resonance pH Sensing via SABRE-SHEATH. ACS Sensors 2016, 1 (6), 640–644. [PubMed: 27379344]

(33). Barskiy D. a.; Kovtunov KV; Koptyug IV; He P; Groome K. a.; Best Q. a.; Shi F; Goodson BM; Shchepin RV; Coffey AM; et al. The Feasibility of Formation and Kinetics of NMR Signal Amplification by Reversible Exchange (SABRE) at High Magnetic Field (9.4 T). J. Am. Chem. Soc 2014, 136 (9), 3322–3325. [PubMed: 24528143]

(34). Pravdivtsev AN; Yurkovskaya AV; Petrov PA; Vieth H-M; Ivanov KL Analysis of the SABRE (Signal Amplification by Reversible Exchange) Effect at High Magnetic Fields. Appl. Magn. Reson 2016, 47 (7), 711–725.

(35). Pravdivtsev AN; Yurkovskaya AV; Zimmermann H; Vieth H; Ivanov KL Transfer of SABRE-Derived Hyperpolarization to Spin-1/2 Heteronuclei. RSC Adv 2015, 5 (78), 63615–63623.

(36). Roy SS; Norcott P; Rayner PJ; Green GGR; Duckett SB A Simple Route to Strong Carbon-13 NMR Signals Detectable for Several Minutes. Chem. - A Eur. J 2017, 23 (44), 10496–10500.

(37). Barskiy DA; Kovtunov KV; Koptyug IV; He P; Groome K. a.; Best Q. a.; Shi F; Goodson BM; Shchepin RV; Truong ML; et al. In Situ and Ex Situ Low-Field NMR Spectroscopy and MRI Endowed by SABRE Hyperpolarization. ChemPhysChem 2014, 15 (18), 4100–4107. [PubMed: 25367202]

(38). Truong ML; Shi F; He P; Yuan B; Plunkett KN; Coffey AM; Shchepin RV; Barskiy DA; Kovtunov KV; Koptyug IV; et al. Irreversible Catalyst Activation Enables Hyperpolarization and Water Solubility for NMR Signal Amplification by Reversible Exchange. J. Phys. Chem. B 2014, 118 (48), 13882–13889. [PubMed: 25372972]

(39). Nelson SJ; Kurhanewicz J; Vigneron DB; Larson PEZ; Harzstark AL; Ferrone M; Criekinge M. Van; Chang JW; Park I; Reed G; et al. Metabolic Imaging of Patients with Prostate Cancer Using Hyperpolarized [1–13C]Pyruvate. Sci Transl Med 2013, 5 (198), 198ra108.

(40). Theis T; Truong M; Coffey AM; Chekmenev EY; Warren WS LIGHT-SABRE Enables Efficient in-Magnet Catalytic Hyperpolarization. J. Magn. Reson 2014, 248, 23–26. [PubMed: 25299767]

(41). Shchepin RV; Barskiy DA; Mikhaylov DM; Chekmenev EY Efficient Synthesis of Nicotinamide-1–15N for Ultrafast NMR Hyperpolarization Using Parahydrogen. Bioconjug. Chem 2016, 27 (4), 878–882. [PubMed: 26999571]

(42). Kovtunov KV; Kovtunova LM; Gemeinhardt ME; Bukhtiyarov AV; Gesiorski J; Bukhtiyarov VI; Chekmenev EY; Koptyug IV; Goodson B Heterogeneous Microtesla SABRE Enhancement of 15N NMR Signals. Angew. Chemie Int. Ed 2017, 56, 10433 –10437.

(43). Shi F; Coffey AM; Waddell KW; Chekmenev EY; Goodson BM Heterogeneous Solution NMR Signal Amplification by Reversible Exchange. Angew. Chemie - Int. Ed 2014, 53 (29), 7495–7498.

(44). Haase A; Frahm J; Matthaei D; Hanicke W; Merboldt KD FLASH Imaging. Rapid NMR Imaging Using Low Flip-Angle Pulses. J. Magn. Reson 1986, 67 (2), 258–266.

(45). Buljubasich L; Franzoni MB; Munnemann K Parahydrogen Induced Polarization by Homogeneous Catalysis: Theory and Applications. Top. Curr. Chem 2013, 338, 33–74. [PubMed: 23536243]

(46). Burueva DB; Romanov AS; Salnikov OG; Zhivonitko VV; Chen Y-W; Barskiy DA; Chekmenev EY; Hwang DW-H; Kovtunov KV; Koptyug IV Extending the Lifetime of Hyperpolarized Propane Gas Via Reversible Dissolution. J. Phys. Chem C 2017, 121, 4481–4487.

(47). Haase A; Frahm J; Matthaei D; Hanicke W; Merboldt K-D FLASH Imaging. Rapid NMR Imaging Using Low Flip-Angle Pulses. J. Magn. Reson 1986, 67 (2), 258–266.

(48). Schmidt AB; Berner S; Schimpf W; Müller C; Lickert T; Schwaderlapp N; Knecht S; Skinner JG; Dost A; Rovedo P; et al. Liquid-State Carbon-13 Hyperpolarization Generated in an MRI System for Fast Imaging. Nat. Commun 2017, 8, 14535. [PubMed: 28262691]

(49). Wang J; Kreis F; Wright AJ; Hesketh RL; Levitt MH; Brindle KM Dynamic 1 H Imaging of Hyperpolarized [1– 13 C] Lactate In Vivo Using a Reverse INEPT Experiment. Magn. Reson. Med 2017, DOI 10.1002/mrm.26725.

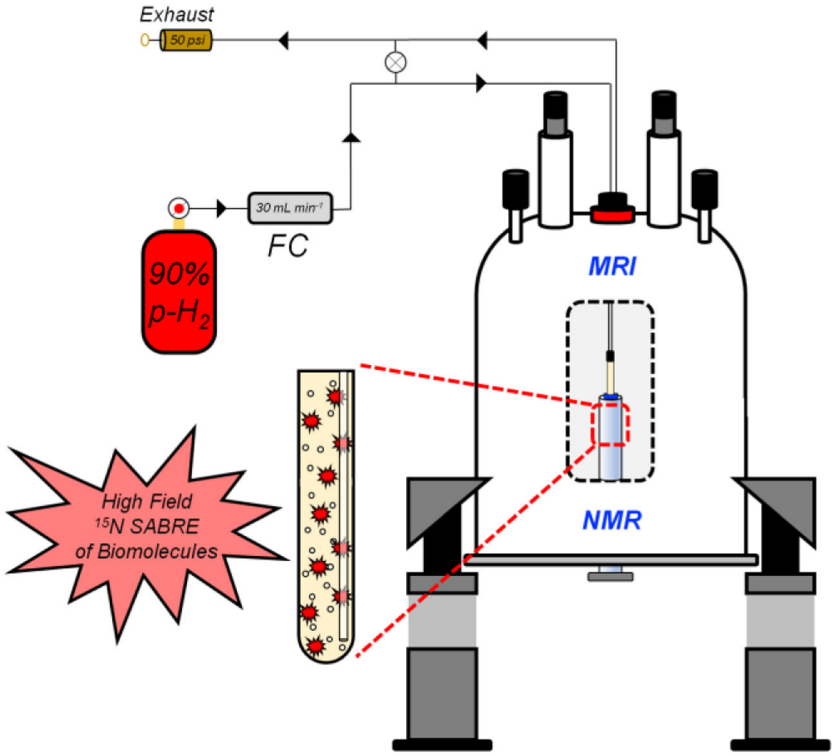

Figure 1.
Experimental setup for the spontaneous transfer of spin order from *para*-H_2-derived protons to ^{15}N nuclei.

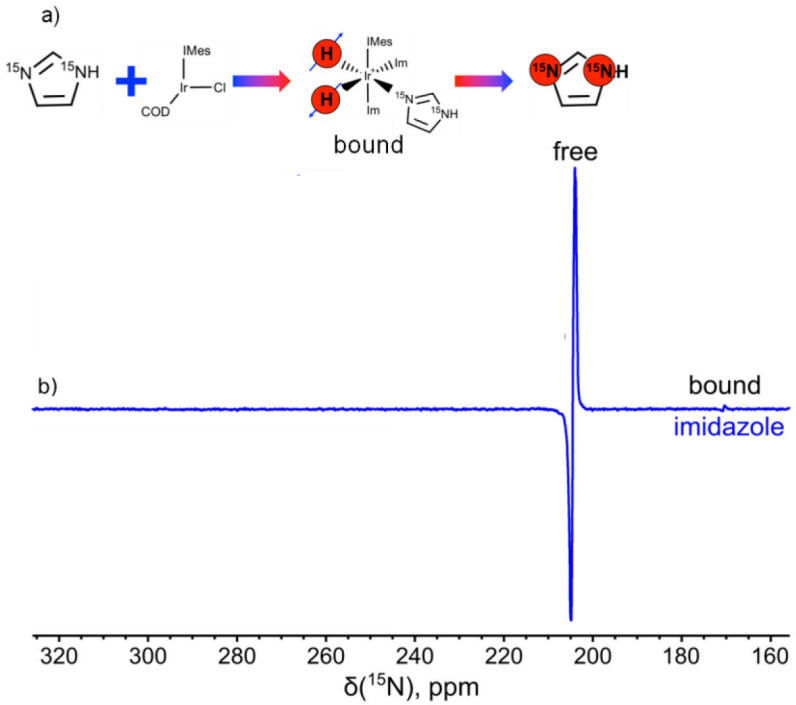

Figure 2.

a) Schematic depicting SABRE catalyst activation and parahydrogen / substrate exchange on the Ir hexacoordinate complex, resulting in imidazole-$^{15}N_2$ hyperpolarization. b) Enhanced ^{15}N NMR spectrum recorded during *in situ para*-H_2 bubbling (i.e. with bubbling occurring while the sample is within a 7 T NMR spectrometer) through a methanol-d_4 solution containing activated 10 mM Ir hexacoordinate catalyst and 100 mM ^{15}N-enriched imidazole-$^{15}N_2$. The signal enhancement for hyperpolarized imidazole was about 120. The spectrum is recorded with 32 acquisitions, with 1 s repetition time between successive scans (total acquisition time: 32 s).

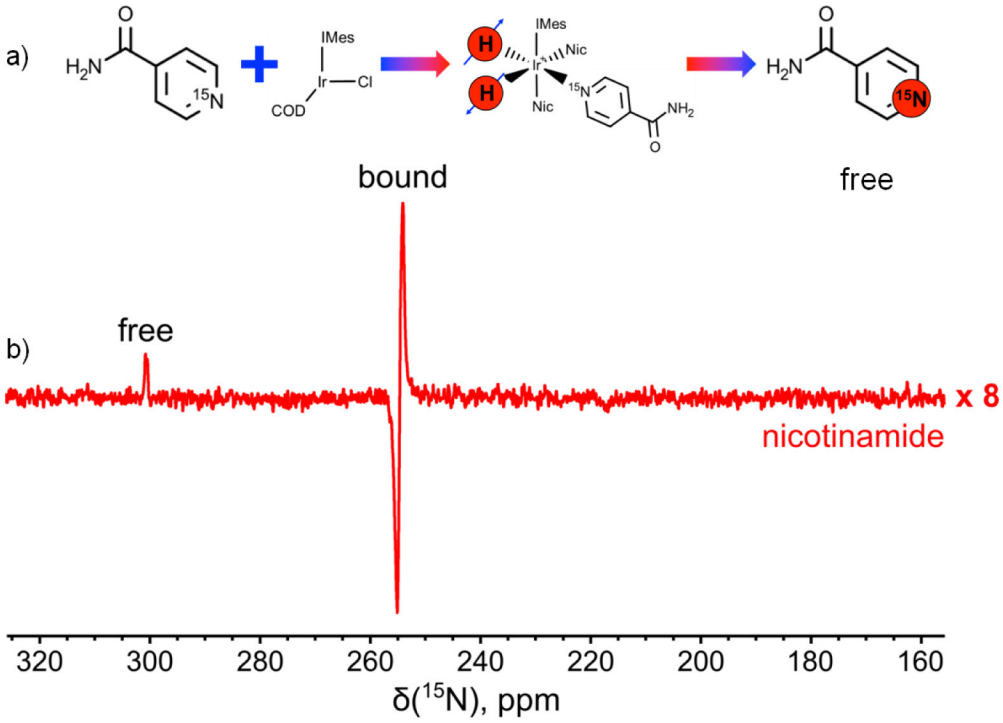

Figure 3.

a) Schematic depicting SABRE catalyst activation and parahydrogen / substrate exchange on the Ir hexacoordinate complex, resulting in nicotinamide-^{15}N hyperpolarization. b) ^{15}N NMR spectrum recorded *in situ* in a 7 T NMR spectrometer during parahydrogen bubbling through methanol-d_4 solution containing activated 10 mM Ir hexacoordinate catalyst and 100 mM ^{15}N-enriched nicotinamide. The signal enhancement for hyperpolarized bounded nicotinamide was about 100. The spectrum is recorded with 32 acquisitions, with 1 s repetition time between successive scans (total acquisition time: 32 s).

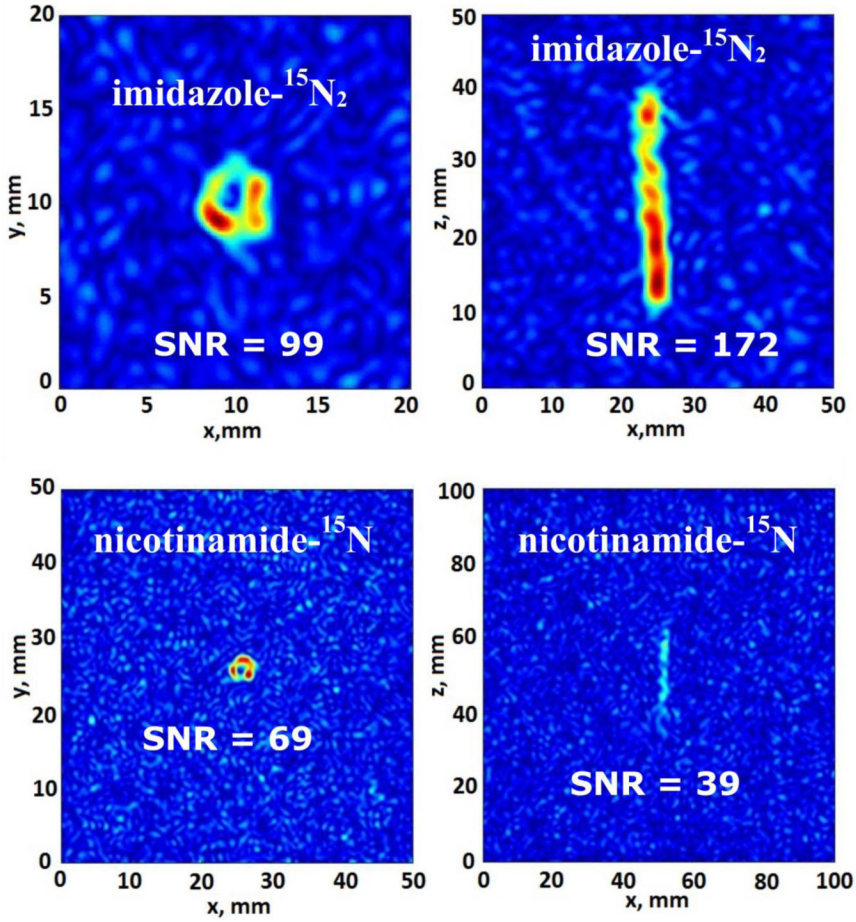

Figure 4.

^{15}N MRI of HP imidazole-$^{15}N_2$ (top) and nicotinamide-^{15}N (bottom) hyperpolarized by the HF-SABRE approach, wherein parahydrogen was bubbled continuously through the imidazole-$^{15}N_2$ solution in a 5 mm NMR tube placed in the high magnetic field (9.4 T) of a MRI scanner (parahydrogen flow was 30 sccm). ^{15}N MR images of ^{15}N HP molecules were acquired using the standard FLASH pulse sequence with an echo time of 6.0 ms and 32 acquisitions during *para*-H_2 bubbling. Images at left are cross sections taken perpendicular to the long NMR tube axis, whereas images are right are taken with the imaging plane parallel to the long axis of the NMR tube. The absence of signal in the center of the cross-sectional images reflects the presence of the PTFE capillary for bubbling *para*-H_2. The fields of view (FOVs) for each projection are presented in each figure; note that the best spatial resolution 0.31×0.31 mm^2 was observed for imidazole-$^{15}N_2$ (*xy* projection). The matrix size was 64×64 and acquisition time was 3 min 25 s for all images.

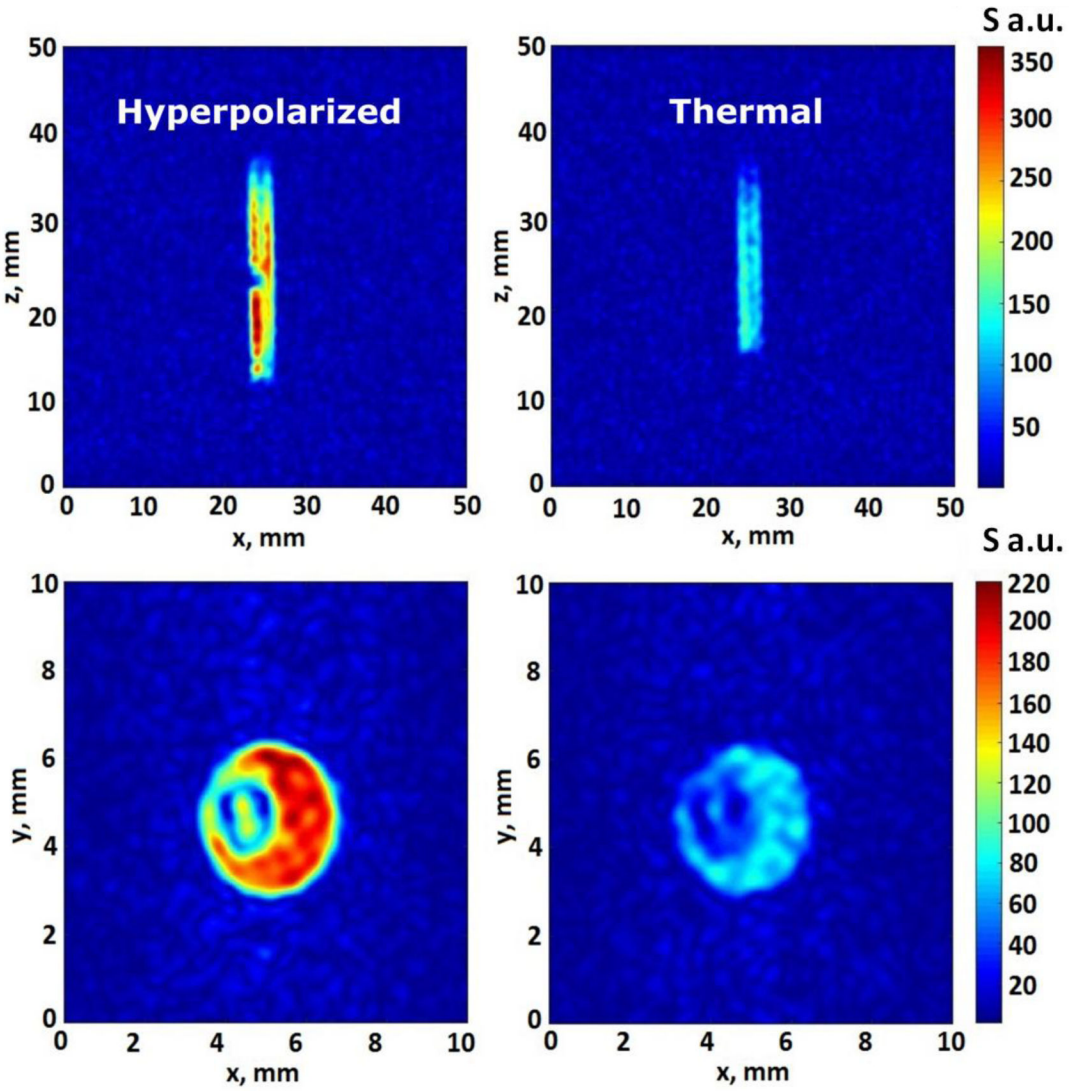

Figure 5.

^{1}H MR images of HF-SABRE hyperpolarized imidazole-$^{15}N_2$ (left column) and thermally polarized imidazole-$^{15}N_2$ (right column) recorded using the FLASH pulse sequence with FOV 5 cm × 5 cm for *xz* projection and 1 cm × 1 cm for *xy*, with a slice thickness of 10 cm. The matrix size was 64×64 and the acquisition time was 960 ms for all images. The spatial resolution was 0.16×0.16 mm^2 for the *xz* projection, high enough to visualize the 1/16” o.d. Teflon capillary in the center.

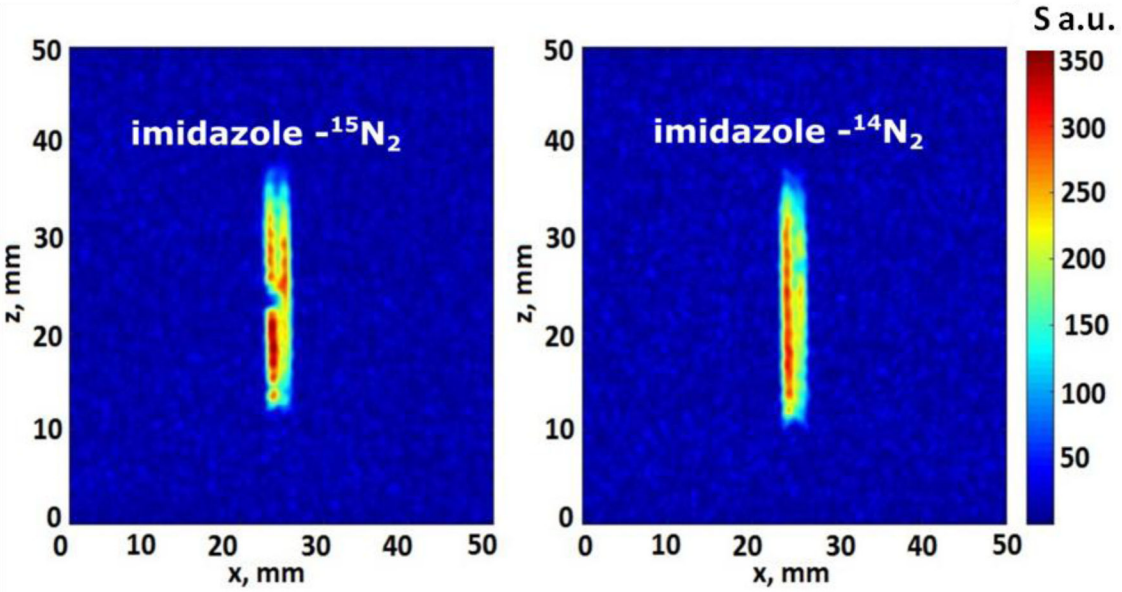

Figure 6.

^{1}H MR images of 5 mm NMR tubes filled with $^{15}N_2$-enriched ("^{15}N", left; same as on Fig. 5) and natural abundant ^{15}N ("^{14}N", right) imidazole hyperpolarized via HF-SABRE. ^{1}H MR images of ^{15}N and ^{14}N imidazole were obtained using the FLASH pulse sequence with a single acquisition and an echo time of 6.0 ms (for both images: FOV: 5×5 cm; matrix size: 64×64; acquisition time: 960 ms).